

time maximum peak load for long operating time. This is extremely useful for testing in blowdown wind tunnels where operating costs can be cut down for short runs. In flight tests, long operating time of the aircraft in a given angle of attack and dynamic pressure band is usually difficult to maintain and a reliable method for estimation of extreme load levels from short time data is very useful.

### Acknowledgments

The authors thank M. Polsenski and N. Tang for their help in reducing wind-tunnel data and to X. L. Shen for supplying the algorithm for the maximum likelihood estimation.

### References

- <sup>1</sup>Lee, B. H. K., and Brown, D., "Wind Tunnel Studies of F/A-18 Tail Buffet," AIAA 16th Aerodynamic Ground Testing Conf., AIAA Paper 90-1432, June 1990; also, *Journal of Aircraft*, Vol 29, No. 1, 1992, pp. 146-152.
- <sup>2</sup>Lee, B. H. K., Brown, D., Zgela, M., and Poirel, D., "Wind Tunnel Investigation and Flight Tests of Tail Buffet on the CF-18 Aircraft," AGARD CP 483, Aircraft Dynamic Loads due to Flow Separation, April 1990.
- <sup>3</sup>Gumbel, E. J., "Statistical Theory of Extreme Values and Some Practical Applications," National Bureau of Standards, Applied Mathematics Series 33, Feb. 1954.
- <sup>4</sup>Jacocks, J. L., "Statistical Analysis of Distortion Factors," AIAA/SAE Eighth Joint Propulsion Specialist Conf., AIAA Paper 72-1100, Nov.-Dec. 1972.
- <sup>5</sup>Jacocks, J. L., and Kneile, K. R., "Statistical Prediction of Maximum Time-Variant Inlet Distortion Levels," AD/A-004 104, Arnold Engineering Development Center, Arnold AFS, TN, Jan. 1975.
- <sup>6</sup>Harley, H. O., "The Modified Gauss-Newton Method for the Fitting of Nonlinear Regression Functions by Least Squares," *Technometrics*, Vol. 3, No. 2, 1961, pp. 269-280.

## Wind-Tunnel Compressor Stall Monitoring Using Neural Networks

Ching F. Lo\* and G. Z. Shi†

University of Tennessee Space Institute, Tullahoma, Tennessee 37388

### Introduction

**R**OTATING stall and stall surge of an axial compressor are two distinct types of aerodynamic instabilities that can severely limit a compressor's performance. Both rotating stall and surge may cause the rotor and stator blades to begin vibrations and the internal compressor temperatures to rise rapidly. The large dynamic stresses on the blades may induce severe mechanical damage. For the case of the C3 rotor blades of 16S compressor, the stall will produce potentially destructive levels of vibratory stress after approximately 10 revolutions (or 1 s) following "onset" of the stall. Rotating stall, which will be the prevalent type in the C-1 compressor of 16T, builds to a peak stress level and the decays in periods of two revolutions (0.2 s). It is apparent that a system is

required that can detect and warn rapidly of the first symptoms of stall and have the capability to activate corrective actions automatically.<sup>1</sup> At the present, the open-loop technique is essentially in the monitoring mode based on observation from many years of experience. The engineer will perform the corrective action to avoid the compressor stall. A closed-loop stall avoidance incorporating a control system to move the compressor operation point away from the stall line is the ultimate goal.

To accomplish detection of stall for compressor requires speed and an automatic process for both open-loop and closed-loop modes. The neural network is a new information processing technology to classify data, process signals, and model and forecast events. The performance of neural networks in the task of classifying data has speed, accuracy, and high noise tolerance; therefore, neural networks techniques are suitable and selected in the present study to detect and monitor compressor instabilities.

### Compressor Stall Monitoring

Stall monitoring for the compressor in the Arnold Engineering Development Center (AEDC) 16-Foot Transonic/Supersonic (16T/S) wind tunnel is investigated. The primary monitoring data are based on the time traces of rotor blade stresses during the operation of 16T/S compressors. The sensor data are recorded in the Compressor Monitoring System disk records and Compressor Monitoring Room oscillograph traces. Some typical rotor/stator stress data are recorded as oscillograph traces, as shown in Fig. 1. An early stall warning and detection expert system is to be constructed utilizing these time traces data and other auxiliary parameters.

### Testing Data Acquisition and Simulator

The data of normal runs for rotors and stators of Compressor C-1 of 16T at AEDC were recorded for various flow conditions. The flow Mach numbers covered include 0.6, 0.9, and 1.2. The original data from stress sensors were recorded

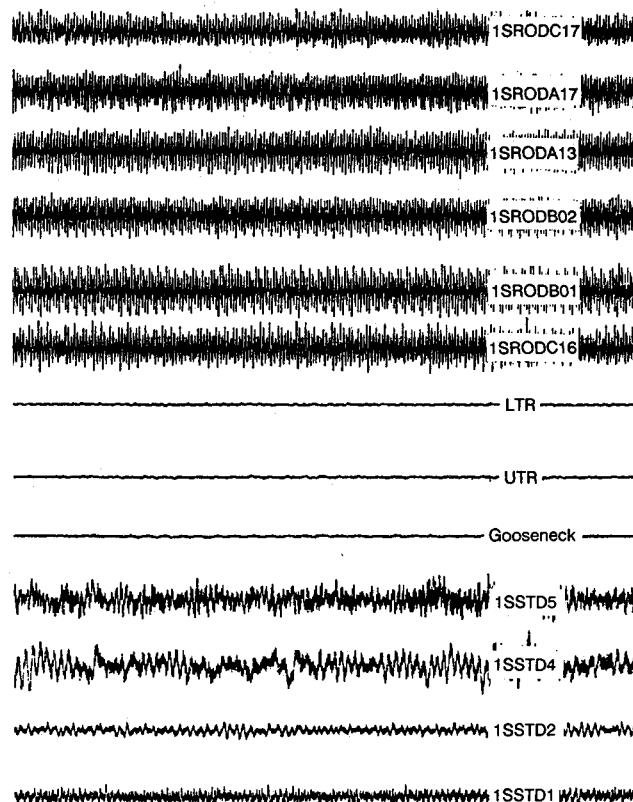
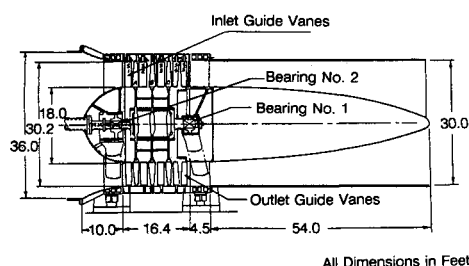


Fig. 1 Typical C-1 compressor stress traces.

Presented as Paper 91-2500 at the AIAA/SAE/ASME 27th Joint Propulsion Conference, Sacramento, CA, June 24-26, 1991; received July 20, 1991; revision received Oct. 5, 1991; accepted for publication Oct. 6, 1991. Copyright © 1991 by the American Institute of Aeronautics and Astronautics, Inc. All rights reserved.

\*Professor of Aerospace/Mechanical Engineering. Member AIAA.

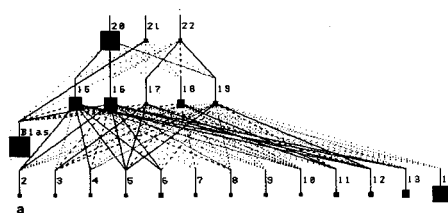
†Research Engineer, CSTAR. Member AIAA.



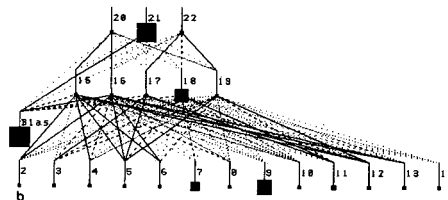
## Design Conditions

Tip Speed 942 ft/sec (absolute)  
 Hub Speed 565 ft/sec (absolute)  
 Design Pressure Ratio 1.385  
 Design Inlet Volume Flow 200,000 cfs  
 Flow Coefficient 0.47  
 Work coefficient 0.308  
 Inlet Axial Velocity 42 ft/sec

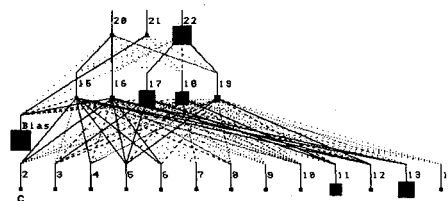
Fig. 2 Dimensions for compressor C-1.



a) Rotating stall



b) Rotor A, normal run



c) Rotor C, normal run

Fig. 5 Three-layer back-propagation network for rotor blade rows A and C.

on magnetic tape in analog format. The rotor and stator locations of Compressor C-1 are shown in Fig. 2.

The analog data were converted to digital format by a commercial program and the spectrum analysis in frequency domain was also carried out by the program. With the output binary data, a program for data reading and plotting was implemented on the PC. The resulted typical frequency spectrum data from the spectrum analysis for A13 (for rotor A and sensor 13) and C17 at Mach number 0.6 are shown in Fig. 3.

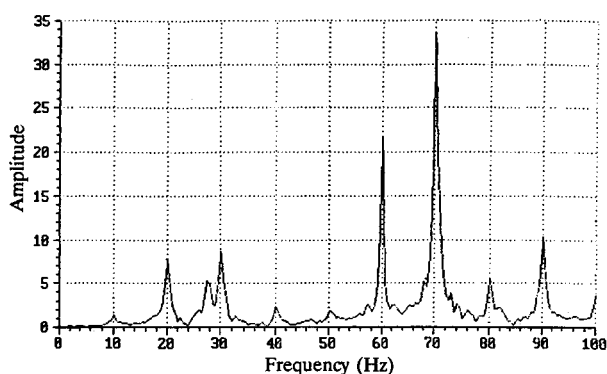
For the neural network process, it is required to acquire sufficient data samples under normal and abnormal operating conditions, especially under stall conditions. Because operation of 16T/S compressors is usually under normal conditions, stress data for the normal condition are relatively easy to acquire. On the other hand, the data under stall condition are very limited. The alternative is to create a numerical simulator that may provide the stall dynamic stress data. It is clear that this simulator is needed to generate stall conditions data, which otherwise would not be available. The rotational stall data have been simulated, as shown in Fig. 4, because the test data are not available at this time.

## Neural Network Architecture

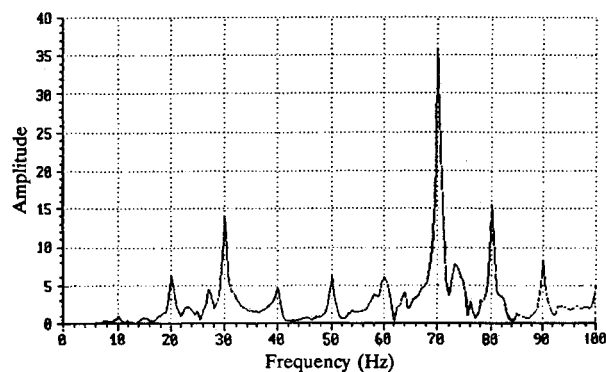
A three-layer back-propagation (BP) network<sup>2</sup> has been selected and implemented in a commercial program for the present study. Multilayer BP networks have been studied extensively and are used widely for pattern classification by the hetero-association memory. Multilayer networks are able to classify nonlinearly separable classes. Back-propagation is the technique selected to solve the current problem. In the present case, a three-layer (input layer, hidden layer, and output layer) network is utilized. The input layer takes the peak amplitude of stress frequency spectrum as feature inputs. Five processing elements (nodes) are selected in the hidden layer. There are three output units representing rotating stall, normal run for Rotor A, and normal run for Rotor C.

## Neural Network Results

All test data have been classified correctly after the training process with the available testing and simulated data. If the



a) Rotor C, sensor C17, M = 0.6



b) Rotor A, sensor A13, M = 0.6

Fig. 3 Typical frequency spectrum data plot.

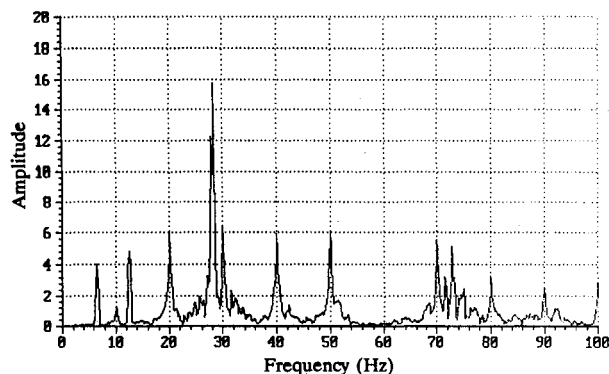


Fig. 4 Simulated frequency spectrum data for rotational stall.

original training data are representative of the underlying distribution, then this test shows quite excellent performance. The graphic display for the results shown in Fig. 5 represents a three-layer network. The size of the rectangular symbols represents the magnitude of the value of each node. The size of output layer symbol 20 in Fig. 5a indicates that this result is a rotating stall condition. The results of a normal run for Rotor-A and Rotor-C are shown by the size of symbols 21 and 22 in Fig. 5b and 5c, respectively.

A monitoring expert system has been designed to assist the operators to monitor the compressors. The expert system consists of three major subsystems: knowledge-based diagnostic subsystem; neural network subsystem; and graphical user interface. The prototype system has been initiated for a complete compressor monitoring system in which several software packages are integrated.

### Conclusions

The feasibility of neural networks to detect the compressor stall has been demonstrated. The selection of features from the blade strain gage data is critical to the successful detection of rotating stall and normal run. The integration of neural network and expert system is a powerful tool for compressor stall monitoring.

### Acknowledgments

This work was supported by AEDC/AF and NASA/Ames Research Center under Grant NAG2-596 and by the University of Tennessee—Calspan Center for Space Transportation and Applied Research under NASA Grant NAGW-1195. The authors thank Carlos Tirres and U. G. Nordstrom of AEDC for their guidance. Frank W. Steinle of NASA Ames was the technical monitor.

### References

- <sup>1</sup>Garnier, V. H., Epstein, A. H., and Greitzer, E. M., "Rotating Waves as a Stall Inception Indication in Axial Compressor," American Society of Mechanical Engineers Paper 90-GT-156, June 1990.
- <sup>2</sup>Rumelhart, D. E., Hinton, G. E., and Williams, R. J., "Learning Internal Representations by Error Propagation," *Parallel Distributed Processing*, edited by D. E. Rumelhart and J. L. McClelland, Vol. 1, MIT Press, Cambridge, MA, 1987, pp. 318–362.

## Effect of a Nose-Boom on Forebody Vortex Flow

T. Terry Ng\*

University of Toledo, Toledo, Ohio 43606

### I. Introduction

At high angles of attack, the sensitivity of the leeward vortices of a slender forebody to external disturbances is well documented. One source of such disturbances on many existing aircraft configurations is the nose-boom. Studies have showed that the wake of a nose-boom can influence substantially the overall forebody flow. There are, however, conflicting reports of increases (e.g., Refs. 1 and 2) and reductions (e.g., Refs. 3 and 4) of the zero-sideslip forebody vortex

asymmetry and sideforce magnitude. The objective of the present water tunnel study is to provide information that may lead to a better understanding of the effect of the nose-boom on forebody vortex flow. Four different models were used to study in detail the interaction between the forebody vortex flow and the nose-boom wake flow. Specifically, the study would try to establish conditions under which the nose-boom would increase or decrease the zero-sideslip asymmetric sideforce.

### II. Experimental Setup

The experiment was conducted in the Eidetics 2436 Flow Visualization Water Tunnel.<sup>5</sup> Two forms of visualization were performed 1) off-surface dye visualization; and 2) surface dye-visualization. Details of the techniques are described in Ref. 5. Three F-16 models were used: a 1/20th-scale full model (model 1; total length = 75.81 cm, including a 3.29-cm nose-boom); the 1/10th-scale forebody section model (model 2; total length = 84.14 cm, including a 5.72-cm nose-boom); and a 3/10th-scale nose-tip model (model 3; total length = 57.86 cm, including a 19.76-cm nose-boom). Models 1 and 2 were tested with and without the standard nose-boom. The primary advantage of using three different models is that the scale of each one can be tailored for specific purposes. In particular, the full model was for visualization of the overall flow and interaction between vortices and various parts of the aircraft configuration. The forebody-section model was used for detailed visualization of the forebody vortices. The nose-tip model was for detailed visualization of the flow at the nose-tip region. One drawback of using different models, however, was that results of the three models would not be identical due to the sensitivity of the forebody flow to even minute physical differences between the models. The difference in Reynolds number introduced further dissimilarities. To a certain degree, this may restrict direct comparisons of the results. Additional tests were performed on a 6% scale F/A-18 forebody section model (model 4; length = 60.2 cm without the nose-boom) with a 3.61-cm-long and 0.32-cm-diam cylindrical nose-boom. The baseline model without the nose-boom had been studied extensively.<sup>5</sup>

Tests for the F-16 models were conducted for angles of attack from 15–60 deg, mostly at  $\beta = 0$  deg and in 5-deg increments. For the F/A-18 model, tests were conducted for angle of attack from 15–65 deg, again in 5-deg increments. The tests were conducted at flow speeds from 5.1–10.2 cm/s, corresponding to a Reynolds number range of about  $0.47 \times 10^3$  to  $0.94 \times 10^3$  per cm. The low-test Reynolds number ensured the flow to be laminar before separation.

### III. Results and Discussions

Results of the F-16 models 1 and 2 show that the nose-boom strongly affects the forebody vortex asymmetry. Without the nose-boom, the forebody flows over both models remain visually symmetric from  $\alpha = 15$  to 60 deg. The effect of the nose-boom is strongly dependent on the angle of attack. The forebody vortex flow for model 1 with the nose boom becomes visibly asymmetric for  $\alpha$ 's above  $\sim 45$  deg. The orientation of the forebody vortices and the degree of asymmetry is dependent on the angle of attack. The vortices can switch between "left-vortex-high" and "right-vortex-high" orientations through the angle of attack range. Initially, the degree of asymmetry increases with the angle of attack. Further increasing the angle of attack, however, eventually leads to a reduction in the vortex asymmetry. Above  $\alpha = 60$  deg the forebody vortices become essentially symmetric, at least in a time-average sense.

Details of the forebody flow are more readily revealed by results of the forebody-section model (model 2). The flows over models 1 and 2 are similar. For model 2, the forebody vortex asymmetry was observed to begin at  $\alpha$  above about 45 deg, reach a maximum at approximately 55 deg, and then reduce significantly when  $\alpha$  increases to 60 deg. At higher

Received June 8, 1991; revision received Sept. 13, 1991; accepted for publication Sept. 13, 1991. Copyright © 1991 by the American Institute of Aeronautics and Astronautics, Inc. All rights reserved.

\*Associate Professor, Department of Mechanical Engineering, Member AIAA.